Proceedings of the 21st ICSMGE, Vienna, Austria, 14 – 19 June 2026. Pistrol, Adam & Schweiger (eds.)
Published by: ÖGG, Austrian Society for Geomechanics, Salzburg, Austria, ISBN 978-3-9503898-4-5
https://doi.org/10.53243/ICSMGE2026-1609

Soil nonlinearity effect on dynamic responses of multi-degree-of-freedom structures supported by shallow foundation: centrifuge modelling

Seong Jin Park, **Yun Wook Choo**
Kongju National University, Korea, Republic of (South Korea); ywchoo@kongju.ac.kr

ABSTRACT: This study aims to address the soil nonlinearity effect on the dynamic response of single- and multi-degree-of-freedom structures with varying periods involved with soil-foundation-structure interaction. Dynamic centrifuge tests were performed, using an in-flight earthquake simulator to simulate the dynamic response of single-, two-, and three-degree-of-freedom structures supported by shallow foundations installed on sandy soils with a relative density of 77 to 80% and subjected to a total of five real earthquake records, including Northridge, Kobe, and so on. The effect of SFSI on the dynamic responses of the structures was analyzed from acceleration signals of accelerometers buried in the ground and attached to the structure. Frequency domain decomposition (FDD) method was utilized to accurately analyze the natural frequencies of the structures on the shallow foundations and ground. The FDD method successfully to separate the modes of the ground and the structure. The period lengthening phenomenon of the structure was clearly observed due to the soil-foundation-structure interaction effect of shallow foundation, presenting the natural period of the ground decreases with the successive shaking events. On the other hand, the natural period of the structures on shallow foundations and ground tends to increase as the number of shaking events and bedrock peak ground acceleration increases. The period lengthening ratio of the structures was calculated and comparted to that calculated by ASCE 7-22, addressing the change in the non-linearity factor of soil dynamic property. The comparison confirms that the nonlinearity factor by the standard overestimates the soil nonlinearity under weak earthquake involved with small strain in the soil layer.

KEYWORDS: SFSI, Period Lengthening, Frequency domain decomposition.

1 INTRODUCTION

Dynamic response of structures constructed on the ground are affected during an earthquake due to the interaction of the soil-foundation-structure interface. Soil-foundation-structure interaction (SFSI) is a very important concept in seismic design. This interaction induces the rocking motion of the foundation, leading to a variation in dynamic response (i.e. natural periods) of the system. On the other hand, this rocking also dissipates the dynamic energy transferred to the structure system through the foundation and ground mitigate possible internal damage structural members in the system (Anastasopoulos et al. 2010), alternatively proposing a new design concept for the foundation considering rocking motion.

The natural period of a structure has been emphasized as a very important factor in seismic design, and it is usually calculated by a modal analysis of the structure under fixed-end conditions. However, actual structures are constructed in soil which is more flexible than the fixed bottom boundary condition and may have different stiffness depending on different support types (Veletsos and Meek, 1974). In addition, SFSI alters the dynamic response of the structure by involvement of rocking into translational motions of the structure and foundation. Therefore, the structure period is varied due to this soil-foundation-structure system, and this is one of the main effects of SFSI as period lengthening (Pecker, 2004; Anastasopoulos et al., 2012; Deng and Kutter, 2012; Gazetas et al., 2013; Deng, Kutter and Kunnath, 2014; Gazetas, 2015; Kim et al., 2015; Selvarajah and Gajan, 2015; Deviprasad and Dodagoudar, 2020; Kiani and Emami, 2024).

The American Society of Civil Engineers (ASCE), Federal Emergency Management Agency (FEMA), and National Institute of Standards and Technology (NIST) present seismic design codes and guidelines based on SFSI (FEMA, 2000; NIST, 2012; ASCE, 2022). In addition, a reduction coefficient (I_0) of the shear modulus as a function of the maximum ground acceleration (PGA) at the surface was suggested to consider the nonlinear behavior of the soil due to large deformation induced by strong earthquake motions, and the influence depth of the soil underneath the foundation was recommended to be upto half of the foundation width.

Most of the previous studies have been conducted on single-degree-of-freedom structures, and Ko et al. (2019) found that I_0 is overestimated at relatively low strain ranges (i.e., sections with small PGA at surface). Therefore, this paper investigated the period lengthening ratio (PLR) and reduction coefficient (I_0) by performing dynamic centrifuge tests on single-degree-of-freedom and multi-degree-of-freedom structures supported by shallow foundation installed on a sandy layer.

2 CENTRIFUGE TEST

This study was conducted using a geotechnical centrifuge at the Korea Advanced Institute of Science and Technology (KAIST), as detailed by Kim et al. (2013). The ground was constructed in an equivalent shear beam (ESB) container, and the prototype size of the constructed soil model was 50.4 m × 37.8 m × 36.0 m (L×B×H). The earthquakes were simulated using a one-dimensional shaking table (Zeng and Schofield, 1996). The model ground, composed of silica sand, was prepared using the air pluviation method to achieve a relative density of 77%.

Accelerometers and bender elements were embedded in the sand model layer during ground preparation to monitor dynamic responses during shaking. The models of soil and structure were designed applying a scaling ratio of 1/60 (Schofield, 1980), and the overall test setup is summarized in Table 1. The structure's cross-sectional details are shown in Figure 1 and Table 2 lists the corresponding structural properties which is model scale at 1 g.

The input motions included Sweep, Resweep, Northridge-SM, Kobe, Artificial, Northridge-CIT, and Chuetsu records. Each motion was applied with gradually increasing amplitudes up to a peak ground acceleration (PGA) of 0.22g. The tests with three structures with different degrees of freedoms were repeatedly installed, excited, and replaced on the same soil model, by changing the structures at 1g condition.

3 RESULT AND DISCUSSION

3.1 *Ground period*

The ground and structure period were analyzed applying multiple methods: response spectrum (RS), fast Fourier

transform (FFT), ratio of response spectrum (RRS), ratio of fast Fourier transform (RFFT) and frequency domain decomposition (FDD). Acceleration data measured by accelerometers embedded in the ground to calculate the natural periods of the ground and the structures were utilized. Frequency domain decomposition (FDD) is one of the most widely used techniques for identifying the modal parameters of a structure through system identification using only output response records (Brincker, 2000; Zhang and Andersen, 2000).

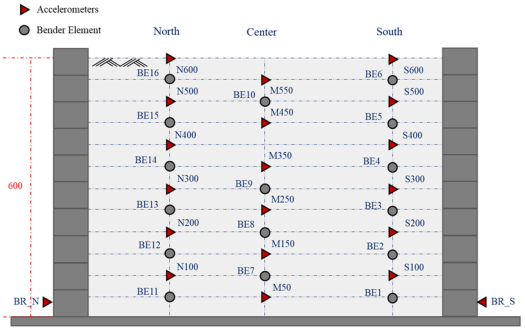

Figure 1. Centrifuge test cross section (A1-1).

Table 1. Test Information.

Test ID	Stucture Condition	Realative Density	Description
A1-1	N/A	77	Free field
A1-2	SDoF	78	single-degree-of-freedom structure (shallow foundation)
A1-3	2DoF	79	two-degree-of-freedom structure (shallow foundation)
A1-4	3DoF	80	three-degree-of-freedom structure (shallow foundation)

Table 2. Model structure properties at model scale.

	SDoF	2DoF	3DoF
Structure	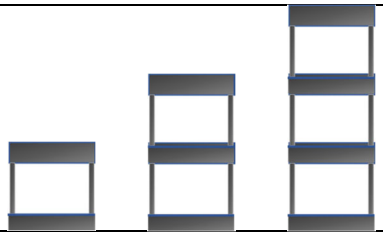		
Lumped mass	0.15 x 0.15 x 0.01 ($L \times W \times d$)		
Leg	0.109 x 0.15 x 0.003 ($H \times W \times t$)		
Foundation	0.15 x 0.15 x 0.01 ($L \times W \times d$)		
Mass (kg)	1.480	2.352	2.352
Effective mass m_s (kg)	0.7759	1.5543	1.5543
Column stiffness, k (N/m)	430,948	430,948	430,948
Fundamental period, Numerical Analysis T_s (s)	T_1= 0.008	T_1= 0.013	T_1= 0.019

The ground and structure periods were estimated by cross-validation with the above-mentioned methods: RS, RRS, FFT, RFFT, and FDD.

Figure 2 is the ground period of the free field condition test (A1-1). The red circle marker in Figure 2 is the calculated ground period, the blue rhombus and dark blue triangle are T_{g0} and T_{g30} on the primary axis, respectively, and the white circle marker is the PGA of the input earthquake wave on the secondary axis. The ground period ranges from 0.63 s to 0.78 s. T_{g0} and T_{g30} were calculated from the shear wave velocities measured by a bender element embedded in the ground within different depth. T_{g0} is done with the V_s profile for the entire layer (36 m in prototype) but T_{g30} is done for the 30-m-depth V_s profile as defined by ASCE. The ground period is within the range between T_{g0} and T_{g30}, which is judged to be properly calculated, and the shear wave velocity of the ground is 174.53 to 199.69 m/s, which is classified as DE class by ASCE. The gray dashed line in Figure 2 is the starting point of each excitation event and tends to decrease as the event number increases. This is a densification effect caused by the vibrations acting on the ground. However, for some earthquake records (e.g., Artificial, Northridge SM), the period also increases with increasing PGA, which is an effect of ground nonlinearity caused by high PGA.

$$V_{s,30} = \Sigma_{i=1}^{n} d_i / \Sigma_{i=1}^{n} \frac{d_i}{v_{si}} \quad (1)$$

Here, n is soil layer number, d_i and v_{si} are the thickness and shear wave velocity of the layer, respectively, ranging from 0 to 30 m

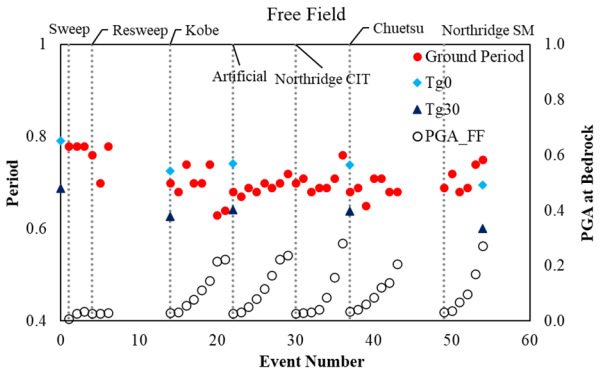

Figure 2. Ground period trend (A1-1) with PGA at bedrock

3.2 *Lengthened period of structure*

Figure 3 shows the ratio of the RS of the top mass of each structure to the RS of the bedrock, and the RRS of all structures is represented by the black dashed line. The red dashed line (denoted NDoF for Natural Period of Fixed condition) is the natural period of the structure in the fixed condition calculated by modal analysis, and the red solid line is the lengthened period of the structure (denoted NDoF as lengthened Period of Flexible condition). The lengthened periods of each structure are 0.67 s for the SDoF structure, 1.46 s for the 2DoF, and 1.94 s for the 3DoF, and are larger than the fixed-end period. This confirms the period lengthening effect of SFSI on the structure, and this effect only applies to the first fundamental period (NIST, 2012).

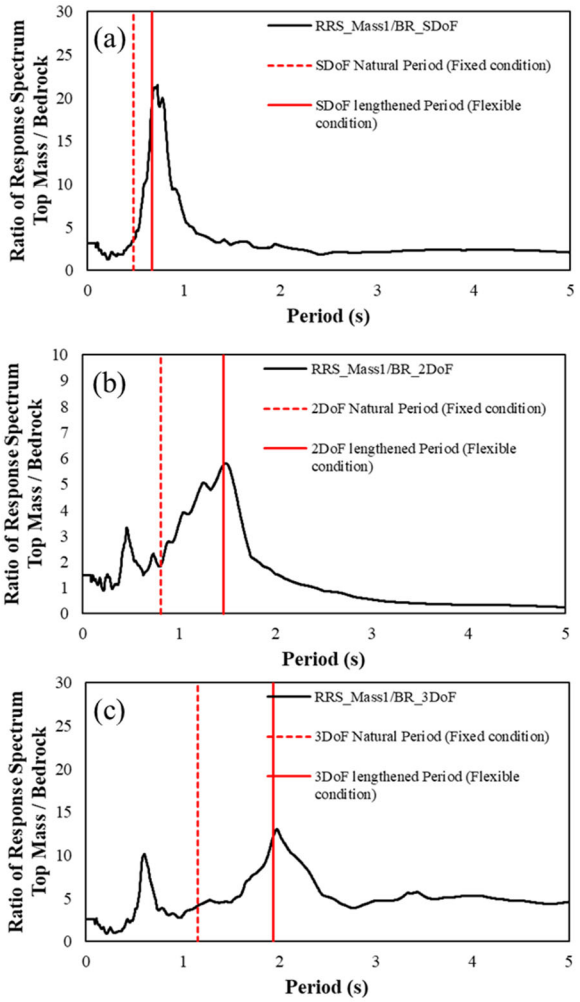

Figure 3. RS of structure with lengthened period (a) SDoF (A1-1, Event 13), (b) 2DoF (A1-2, Event 13) and (c) 3DoF (A1-3, Event 10)

The period of the structure in all tests is as shown in Figure 4. The period tends to increase as the PGA increases due to the period lengthening effect, but the two-degree-of-freedom structural period (black circle marker in Figure 4) decreases in some events. This is believed to be due to the limitation of the rocking motion caused by the decrease in the strength of the foundation subgrade.

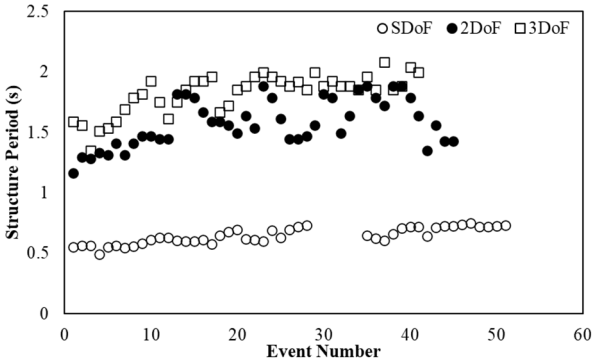

Figure 4. Lengthening period trend

3.3 *Period lengthening ratio*

The period lengthening ratio of the structure used in the test is shown in Figure 5 and the equation is as follows (NIST).

$$PLR = \frac{\tilde{T}}{T} = \sqrt{1 + \frac{k}{k_x} + \frac{kh^2}{k_{yy}}} \quad (2)$$

where $\tilde{T}$ and T are the extended period and natural period, respectively, and k, k_x, and k_{yy} are the structural stiffness, soil horizontal stiffness, and rotational stiffness, respectively.

The above equation can also be applied to the MDoF structure, and the equivalent stiffness in Table 3 was calculated and applied to the MDoF (Zhao and Zhang, 2020).

Table 3. Structure equivalent stiffness (k_{eq}).

Type	Equivalent stiffness
SDoF	25,856,880 N/m
2DoF	19,752,898 N/m
3DoF	14,559,364 N/m

Generally, the PLR increases with the increase of PGA at the surface, with the smallest PLR for SDoF structures with the largest equivalent stiffness. On the other hand, for MDoF structures, the ratio of 2DoF structures is larger than that of 3DoF structures, different from the relationship of equivalent stiffness. This is judged to be the result of the heavier and taller 3DoF structure, which causes lower rocking motion, and the stiffness reduction due to the higher nonlinearity of the subgrade under the 2DoF structure.

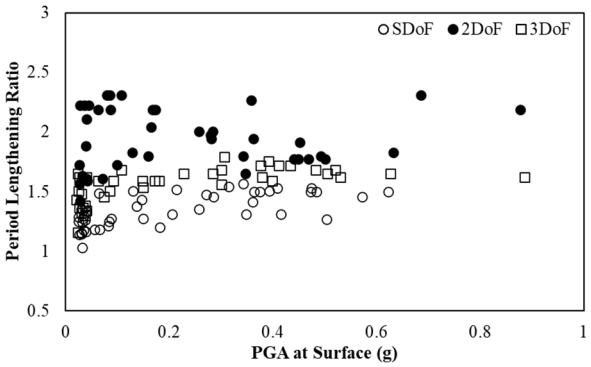

Figure 5. Period lengthening ratio of structure

3.4 *Reduction coefficients I_0 of shear modulus*

The reduction coefficient I0 was calculated by back calculating the equation presented by NIST (Figure 6). For all tests, the reduction coefficient decreases as the surface PGA increases. Consistent with previous studies, the ASCE I_0 is overestimated for all structures with a PGA of less than 0.4 g for the soil in this paper. In addition, there is a trend toward underestimation for PGA greater than 0.4g. Also, as mentioned in Section 3.3 above, it can be observed that the reduction coefficients have the smallest value due to the high nonlinearity of the subgrade under 2DoF.

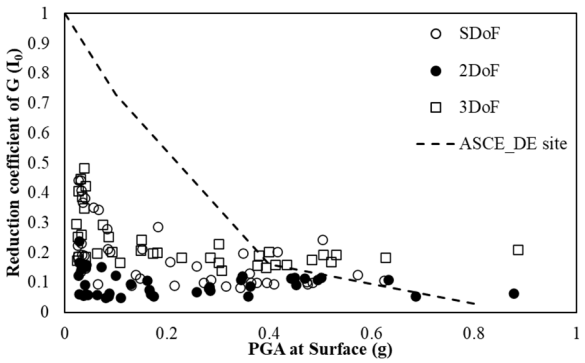

Figure 6. Reduction coefficient of shear modulus (a) SDoF, (b) 2DoF and (c) 3DoF

4 CONCLUSION

Dynamic centrifuge model tests were conducted to study the period lengthening ratio and shear reduction coefficient (I_0) of shallow foundation-supported single- and multi-degree-of-freedom structures considering the soil-foundation-structure interaction.

- The ground period shows a similar trend to the period calculated from the measured shear wave velocity, and it is confirmed that the period increases with the increase of PGA due to the increase of nonlinearity for some earthquake excitations, and the period lengthening effect, which is the main effect of soil-foundation-structure interaction, was observed for all structures.
- The lengthening of the single-degree-of-freedom structure (SDoF) period is the smallest for due to the difference in stiffness, and the largest for the three-degree-of-freedom structure (3DoF). The two-degree-of-freedom structure (2DoF) has the highest period lengthening ratio and the smallest nonlinear reduction coefficient due to the high nonlinearity of the subgrade under foundation.
- The model soil relative density in this study is 77 to 80%, the heights of the model structures are 7.74 m, 14.88 m, and 22.02 m for SDoF, 2DoF and 3DoF structures, respectively, and the foundation width is 9 m. At these conditions, the shear modulus reduction coefficient proposed by ASCE is overestimated in the low strain range and partially underestimated in the high strain range.
- These discrepancies in reduction coefficient can result in incorrect identification of lengthened period and seismic design. However, the ground models used in this test are prepared with uniform silica sand, and the conclusions of this paper are limited to trends for ideal and clean sand. Therefore, further study is suggested for I_0 over a wider range of soil conditions using various methodologies.

5 ACKNOWLEDGEMENTS

This work was supported by the National Research Foundation of Korea (NRF) grant funded by the Korea government (MSIT) (No. RS-2024-00406320).

6 REFERENCES

Anastasopoulos, I., Gazetas, G., Loli, M., Apostolou, M. and Gerolymos, N., 2010. Soil failure can be used for seismic protection of structures. *Bulletin of Earthquake Engineering*, 8(2), pp.309–326. https://doi.org/10.1007/s10518-009-9145-2.

Anastasopoulos, I., Kourkoulis, R., Gelagoti, F. and Papadopoulos, E., 2012. Rocking response of SDOF systems on shallow improved sand: An experimental study. *Soil Dynamics and Earthquake Engineering*, 40, pp.15–33. https://doi.org/10.1016/j.soildyn.2012.04.006.

American Society of Civil Engineers, 2021. *Minimum Design Loads and Associated Criteria for Buildings and Other Structures*. [online] American Society of Civil Engineers. https://doi.org/10.1061/9780784415788.

Brincker, R., Zhang, L. and Andersen, P., 2000. Modal Identification from Ambient Responses using Frequency Domain Decomposition: The International Modal Analysis Conference. *IMAC 18 : Proceedings of the International Modal Analysis Conference (IMAC), San Antonio, Texas, USA, February 7-10, 2000*, pp.625–630.

Deng, L. and Kutter, B.L., 2012. Characterization of rocking shallow foundations using centrifuge model tests. *Earthquake Engineering & Structural Dynamics*, 41(5), pp.1043–1060. https://doi.org/10.1002/eqe.1181.

Deng, L., Kutter, B.L. and Kunnath, S.K., 2014. Seismic Design of Rocking Shallow Foundations: Displacement-Based Methodology. *Journal of Bridge Engineering*, [online] 19(11). https://doi.org/10.1061/(asce)be.1943-5592.0000616.

Deviprasad, B. and Dodagoudar, G., 2020. Seismic response of bridge pier supported on rocking shallow foundation. *Geomechanics and Engineering*, 21(1), pp.73–84.

FEMA, 2000, Prestandard and Commentary for the Seismic Rehabilitation of Buildings, FEMA 356, Federal Emergency Management Agency, Washington, D.C.

Gazetas, G., 2015. 4th Ishihara lecture: Soil–foundation–structure systems beyond conventional seismic failure thresholds. *Soil Dynamics and Earthquake Engineering*, 68, pp.23–39. https://doi.org/10.1016/j.soildyn.2014.09.012.

Gazetas, G., Anastasopoulos, I., Adamidis, O. and Kontoroupi, Th., 2013. Nonlinear rocking stiffness of foundations. *Soil Dynamics and Earthquake Engineering*, 47, pp.83–91. https://doi.org/10.1016/j.soildyn.2012.12.011.

Kiani, K. and Emami, S.M.M., 2024. The effect of infill walls on the fundamental period of steel frames by considering soil-structure interaction. *Earthquakes and Structures*, 26(6), pp.417–431.

Kim, D.-K., Lee, S.-H., Kim, D.-S., Choo, Y.W. and Park, H.-G., 2015. Rocking Effect of a Mat Foundation on the Earthquake Response of Structures. *Journal of Geotechnical and Geoenvironmental Engineering*, [online] 141(1). https://doi.org/10.1061/(asce)gt.1943-5606.0001207.

Kim, D.-S., Kim, N.-R., Choo, Y.W. and Cho, G.-C., 2013. A newly developed state-of-the-art geotechnical centrifuge in Korea. *KSCE Journal of Civil Engineering*, 17(1), pp.77–84. https://doi.org/10.1007/s12205-013-1350-5.

Ko, K.-W., Ha, J.-G., Park, H.-J. and Kim, D.-S., 2019. Investigation of Period-Lengthening Ratio for Single-Degree-of-Freedom Structures Using Dynamic Centrifuge Test. *Journal of Earthquake Engineering*, 25(7), pp.1358–1380. https://doi.org/10.1080/13632469.2019.1576557.

NIST, N., 2012. Soil-structure-interaction for building structures (nist gcr 12-917-21). National Institute of Standards and Technology, Gaithersburg, MD, 20899.

Pecker, A., 2004. Design and Construction of the Rion Antirion Bridge. In: *Geotechnical Engineering for Transportation Projects*. [online] GeoTrans 2004. Los Angeles, California, United States: American Society of Civil Engineers. pp.216–240. https://doi.org/10.1061/40744(154)7.

Selvarajah, P. and Gajan, S., 2015. Rocking shallow foundations as seismic energy dissipaters: Theoretical analyses of experimental findings.

Schofield, A. N., 1980. Cambridge geotechnical centrifuge operations. *Geotechnique*, 30(3), 227-268. https://doi.org/10.1680/geot.1980.30.3.227

Veletsos, A.S. and Meek, J.W., 1974. Dynamic behaviour of building-foundation systems. *Earthquake Engineering & Structural Dynamics*, 3(2), pp.121–138. https://doi.org/10.1002/eqe.4290030203.

Zeng, X. and Schofield, A.N., 1996. Design and performance of an equivalent-shear-beam container for earthquake centrifuge modelling. *Géotechnique*, 46(1), pp.83–102. https://doi.org/10.1680/geot.1996.46.1.83.

Zhao, Y. and Zhang, H., 2020. A simple approach for the fundamental period of MDOF structures.